Biomedical Sciences
2019; 5(3): 27-33
http://www.sciencepublishinggroup.com/j/bs
doi: 10.11648/j.bs.20190503.12
ISSN: 2575-3924 (Print); ISSN: 2575-3932 (Online)

Review Article

Plasmonic Effects in Noble Metal-liquid Metal Based Nanoparticles

Akanksha Bhardwaj, Suram Singh Verma*

Department of Physics, Sant Longowal Institute of Engineering & Technology, Longowal, Punjab, India

Email address:
ssvermaus2001@yahoomail.com (S. S. Verma)
*Corresponding author

To cite this article:
Akanksha Bhardwaj, Suram Singh Verma. Plasmonic Effects in Noble Metal-liquid Metal Based Nanoparticles. *Biomedical Sciences*. Vol. 5, No. 3, 2019, pp. 27-33. doi: 10.11648/j.bs.20190503.12

Received: September 26, 2019; **Accepted**: October 21, 2019; **Published**: October 25, 2019

Abstract: In the era of flexible and foldable devices, liquid metals emerge as a champion because they are being liquid at or near room temperature in addition to having high electrical and thermal conductivities. Plasmonic resonance occurs when conduction band electrons on metal nanoparticle surface collectively oscillates with same frequency as that irradiated light. This plasmonic resonance has attracted great attention because of large electromagnetic field enhancements near metal nanoparticle and the regulating resonance wavelength with change in material, size, shape and surrounding medium of metallic nanoparticle. Incorporation of liquid metal nanoparticles in plasmonics provides unique properties towards sensing (heart rate monitors etc.) which can become wearable. So, developing liquid metal based low-cost and large-scale plasmonic nanostructures may provide more optical efficiencies, fast kinetics, low temperature processing, versatility, easy embedding in structures and stretchy devices. Present work focuses on literature review highlighting the study of optical properties (absorption and scattering efficiencies, LSPR tunability, Figure of Merit (FOM) and Refractive Index Sensitivity (RIS)) of noble metal-liquid metal nanostructures and future scope of the field. Simulations can be performed on the basis of Mie Theory for spherical nanoparticles and by DDA/FDTD method for non-spherical particles or arrays. The results can help to optimize the plasmonic nanostructures of suitable material, size and shape according to the need of application in particular region of EM spectrum.

Keywords: Noble Metals, Liquid Metals, Plasmonics, LSPR, Nanoparticles

1. Introduction

At nanoscale large surface-area to volume ratio is the key feature, so materials compared to their bulk counterpart exhibit different properties be it electric, magnetic, physical or chemical, this change leads to the use of materials in many new ways for practical applications. The fascinating applications includes smart textiles, portable electronic devices etc. This is why nanoplasmonics has been a prime area for research, which studies the confinement of electromagnetic (EM) field in dimensions less than wavelength of light. The resonating interaction of EM light with conducting electrons excitation near metallic surfaces evolves enhanced optical fields which can be applied to highly sensitive devices, efficient solar cells and bio-imaging. The origin of plasmonics dates back to 4^{th} century where gold nanoparticles were used in making glass art works without any knowledge about nanoparticles [1]. The first identification of gold NPs for the 'ruby fluid' was reported in 1857 by Michael Faraday [2]. Gustav Mie was the first who theoretically provided the exact solutions of Maxwell equations and reasons for the red color of colloidal gold and studied the effect of size and surrounding medium on optical properties of nanospheres [3]. Mie theory had wide applicability as one can now calculate the extinction (absorption + scattering) spectra for particle with the input of its dielectric function so further Mie theory was extended for spheroidal (oblate and prolate) shaped nanoparticles [4]. Further many researchers gave algorithms for various shaped NPs.

Understanding of plasmonics requires understanding of Drude Model, Maxwell equations and plasma. The LSPR peak wavelength dependence on dielectric function of medium in functional form is obtained by Drude Model. The analytical frequency-dependent form for $\varepsilon(\omega)$ for electronic structure of

metals:

$$\varepsilon(\omega) = 1-\omega p^2\omega^2+ \gamma^2$$

Here ωp is the plasma is the plasma frequency and γ is the damping constant of the bulk metal. For visible and near-infrared frequencies where the frequency is close to plasma frequency, damping can be neglected as $\gamma \ll \omega p$. Thus, above equation reduce to:

$$\varepsilon\ (\omega) = 1-\omega p^2\omega^2$$

The generalized Drude Theory considers complex dielectric function, written as:

$$\varepsilon\ (\omega)= \varepsilon_1\ (\omega)+ i\,\varepsilon_2\ (\omega)$$

$\varepsilon_1\ (\omega)$ is the real part of the dielectric function which describes the strength of polarization induced by an external electric field and $\varepsilon_2\ (\omega)$ is the imaginary part that shows the losses encountered in polarization of material. At optical frequencies $\varepsilon\ (\omega)$ can be experimentally determined by reflectivity studies of material. Using the equation of $\varepsilon\ (\omega)$ for the resonance condition where $\varepsilon\ (\omega)= -2\varepsilon_m$ the following equation can be obtained:

$$\omega_{max}=\omega_p\sqrt{2\varepsilon_m}+1$$

ω_{max} is the LSPR peak frequency. In terms of wavelength ($\lambda=2\pi c/\omega$) equations becomes, $\lambda_{max}=\lambda_p\sqrt{2}n+1$, ($\varepsilon_m = n^2$, n is the refractive index). λ_{max} is the wavelength corresponding to LSPR peak and λ_p is wavelength for plasma frequency of the bulk metal. This equation shows linear dependence of LSPR peak wavelength on refractive index approximately at optical frequencies which are used in experiments [5].

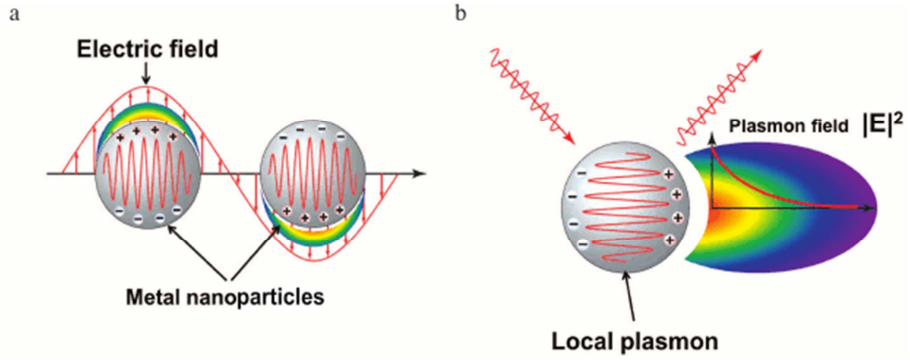

Figure 1. *a) LSPR excitation in metal nanoparticle by electric field of incident light and b) field intensity distribution around a nanoparticle with excited plasmon [Sotnikov, D. V., Zherdev, A. V., & Dzantiev, B. B. (2015). Biochemistry (Moscow), 80 (13), 1820-1832.].*

Plasma is a matter of charged carriers, in same way free electrons oscillate with respect to immobile positive charge near metal surface when interacted with light. The oscillation of free electrons near metallic surface is quantized by a quasiparticle called plasmon, similar to that of photon quantizing light and phonon quantizing mechanical vibration. This collective excitation of free electrons near surface is supported by materials that exhibit a large negative real and small positive imaginary dielectric constant simultaneously. This excitation is known as Surface Plasmon excitation. The interaction of light and metallic surface involves two fundamental plasmonic excitations Surface Plasmon Polaritons (SPPs) and Localized Surface Plasmons (LSPs). SPPs are EM excitations *propagating* at dielectric-conductor interface, while LSPs are the *non-propagating* excitations of conducting electrons of metallic nanostructures. The consequence of LSPs over SPPs is that plasmon resonances can be excited directly by light beams as not in latter's case where phase-matching techniques (like prism coupling or grating) are required for excitations [5]. This LSPR phenomenon is the main cause of strong peaks arising in Surface Enhanced Raman Spectroscopy (SERS) and strong enhancement of local EM field around nanoparticles. Many LSPR based studies have been reported in recent years, Sekhon et al. studied the LSPR based plasmonic properties of Au, Ag and Cu nanoparticles for different shapes and various surrounding medium and found LSPR to be highly sensitive even for a minute change in above said parameters. This sensitivity scopes for bio-sensors and optical sensors devices [6].

Noble metal nanoparticles (Au, Ag) having abundant free electrons, chemical stability and less reactivity, have been widely exploited in this field showing remarkable optical properties based on LSPR. They have shown many applications, Shim et al. reviewed various methods reported for ultrasensitive biodiagonostics using metal NPs, Wu et al. reported improved sensitivity of biosensors by SPR method, Han et al. studied gold nanoparticles in target drug delivery, optical imaging and photoacoustic [7-10]. Many other plasmonics materials are also reported to have the ability to support SPR such as aluminium, gallium, magnesium, indium, copper, palladium, platinum have shown emerging applications for UV plasmonics, gas sensing etc [11-13]. The LSPR phenomena in various applications like highly sensitive nanosensors, plasmonic components and surface-enhanced spectroscopies are largely based on position of LSPR excitation maximum λ_{max}. This resonance peak in excitation due to incident light is strongly reactive to size, shape, surrounding dielectric environment and dielectric properties of nanoparticles. These parameters are explained below:

Size effect: The LSPR peaks depends on particle size, in

quasi-static approximation, LSPR peaks arises due to dipolar plasmon resonance mode. Increasing particle size has shown shift in resonance peaks and also higher multipole mode comes into picture. These resonance modes are explained by an equation [14].

$$\varepsilon_1 = -\{\frac{l+1}{l}\}\varepsilon_s$$

Here l stands for order of resonance mode. For dipole mode l=1, for quadrupole mode l=2, for octupole mode l=3 etc. the multipole mode peaks arise due to unsymmetrical charge distribution of metal NPs. For a NP size upto 25 nm absorption efficiencies dominate the extinction spectra and for larger NP scattering efficiencies contribute more to extinction spectrum.

Shape Effect: The shape of the NP also affects the LSPR peaks, as the resonance peaks depends on dielectric function which also depends on surrounding medium. The real part of dielectric function is given as $\varepsilon_1 = -\frac{(1-L_\gamma)}{L_\gamma}\varepsilon_s$,

ε_s is surrounding dielectric medium and L_γ is depolarizing factor which depends on geometric parameters of metal NP. For spherical NP L=1/3 and only one peak arise, for spheroid NP (prolate and oblate) two peaks are observed based on the oscillation of electron along (longitudinal mode) and perpendicular (transverse mode) to axis. For ellipsoid shaped NP three plasmon modes are observed. The multipole modes for non-spherical shapes are due to edges present in them where electron density is somewhat maximum rather than surface of nanoparticle [15].

Surrounding Medium Effect: The resonant condition for the LSPR to take place according to Mie Theory $\varepsilon(\omega) = -2\varepsilon_s$, shows that real part of dielectric constant of metal NP decreases with increasing wavelength and increase in dielectric of surrounding medium leads to red shift in LSPR wavelength [16].

Plasmonics based on the unique properties offered by materials can be divided into many types such as Semiconductor active Plasmonics that deals with electronic properties at nanoscale for more efficiency of present solar cells, Magneto-Plasmonics is the study based on magnetic and plasmonic properties which shows their potential use in cancer therapy, biomedical imaging etc, liquid plasmonics is integration of plasmonics with liquid metals at room temperature that will be apt for soft electronics. These different properties offer different applications in various fields of science and technology.

2. Liquid Plasmonics

Recent advancements in research and technology demands for devices that can be folded into any shape, this calls for flexibility, portability and reformability of devices. Though thin layers of copper and gold and liquid crystals have been reported for the use in flexible electronics but devices based on these materials are limited by inherent rigidity and increases complexity of metal layers fabrication [17, 18]. Also, there is a chance of cracking due to higher bending or stretching. Smart devices only require small currents so the need is for the materials with extreme flexibility and high electrical conductivity and also appliances based on these materials can conform to skin (deformable surfaces). These desires are fulfilled by liquid phase. Thus, liquid metals having water like viscosities are apt for these devices. The key features of liquid phase like high surface tension, low viscosity, low vapour pressure, self-assembly, coolant at room-temperature can be exploited into plasmonic devices. These features make liquid metals best suited for flexible conductive materials. The basic definition of liquid metals accounts for the metals whose melting point (MP) is near or below room temperature. Liquid metals are known to be either elemental or different metals (post-transition or zinc group metals) alloyed together with low melting point. Mercury (MP is -38.8°C), Gallium (MP is 29.8°C), Cesium (MP is 28.5°C) and Rubidium (MP is 39°C) are the elemental liquid metals. For a comparison the electron density values of these liquid metals and Au & Ag noble metals are given in Table 1 as:

Table 1. *Properties of liquid metals and noble metals in detail.*

Metal	Atomic Number	Electronic Configuration	Atomic mass (g/mol)	Density (kg/m^3)	No. of atoms per unit volume (n_0) =N_A x Density/Atomic Mass (10^{28}/m^3)	Free electron density= n_0 x no of free electrons per atom (10^{28}/m^3)	Bulk Plasma frequency f=9√n Hz (10^{14}Hz)	Surface plasma frequency = f/√2 (10^{14}Hz)
Gallium	31	2, 8, 18, 3	69.72	5907	5.1	15.5	35.43	25.06
Rubidium	37	2, 8, 18, 8, 1	85.467	1530	1.1	1.1	9.44	6.68
Silver	47	2, 8, 18, 18, 1	107.86	10490	5.85	5.86	21.77	15.40
Cesium	55	2, 8, 18, 18, 8, 1	132.90	1873	0.91	0.91	8.58	6.07
Gold	79	2, 8, 18, 32, 18, 1	196.96	19320	5.89	5.89	21.84	15.44
Mercury	80	2, 8, 18, 32, 18, 2	200.59	13593	4.08	8.16	25.71	18.18

The origin of low melting point in liquid metals is discussed on the basis of the valence electrons of metals and the bonding in between electrons. Large number of unpaired electrons and lower degree of ionization in elements leads to low melting point [19]. Hg ($6s^2 5d^{10}$) has completely filled d and s shells, this unique electron configuration strongly resists removal of an electron that results in pseudo noble gas configuration having only weak interactions among valence electrons [20]. Post transition metal Ga ($4s^2 4p^1$) has partially filled p shells resulting in covalent bonding thus featuring high boiling points and low melting points [21, 22].

Mercury over the decades have found many applications in button batteries, as industrial catalyst and in thermostats etc. Liquid gallium has been widely used for higher resolution images of human organs in X-ray scans, in phase change memory devices and in SERS applications [23-25]. Cesium is

known to be immensely used in gas sensing applications, in optical glass and as catalyst promoter etc [26]. The cesium clock is used in Global Positioning System for quantum measurements to maintain accuracy [27]. Also, there is a cancer treatment approach which is known as cesium therapy (or High pH therapy) which involves the usage of cesium chloride (CsCl) salt [28]. Conventional liquid metals have always been ruled out due to their toxicity or reactivity. Since bimetallic core-shell nanostructures have found many applications such as, Ghosh et al. has provided an overview of different classes, properties and synthesis of core-shell nanostructures, Kelly et al. has given basic explanation for influence of particle size, shape and dielectric environment on optical properties of metal nanoparticles [29, 16].

We can use liquid metals in bimetallic (core-shell) nanostructures, where chemical stability can be provided and also noble metal coatings can enhance their plasmonic response as well. Similarly, liquid metal alloys at room temperature (Table 2) can also be explored for their plasmonic properties in association with noble metals.

Table 2. *Composition and melting point of alloyed elements [19].*

Alloy	Element A (%)	Element B (%)	Melting point (°C)
Ga/In	85.8	14.2	15.4
Ga/Sn	91.7	8.3	21.0
Ga/Al	97.6	2.4	25.9
Ga/Zn	96.1	3.9	24.7
Ga/Hg	98.0	2.0	27.0
Ga/Ag	96.4	3.6	26.0

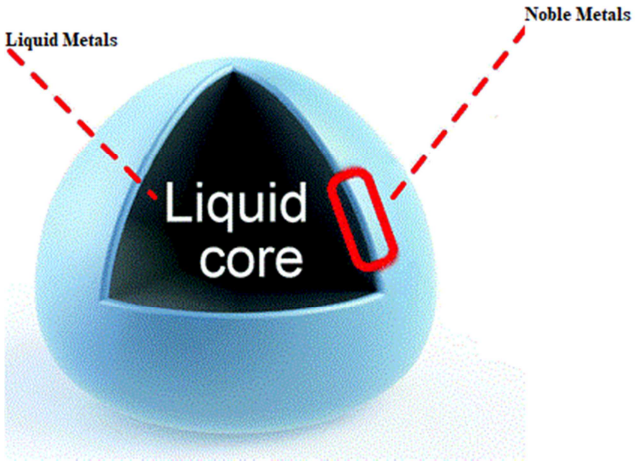

Figure 2. *Noble Metal-Liquid Metal based core-shell nanostructures [19].*

3. Research in Progress

The synthesis and optical properties of liquid metals in plasmonic core-shell nanostructures have been discussed broadly in past decade. Wu et al. studied Ga@Mg core-shell nanoparticles experimentally for their SPR based properties [30]. The red shift in resonance peak was observed with increasing Mg shell thickness keeping the overall nanoparticle size fixed. Tuning the peaks from UV to IR region, results were also confirmed with theoretical calculations by discrete dipole approximation method. Thus, it was found that bimetallic NPs yield tunable SPR which certainly will contribute to the applications of various plasmon resonance frequencies. Tevis et al. demonstrated a low-cost effective approach to synthesize liquid metal nanoparticles in core-shell nanostructures [31]. They used shearing liquid into complex particles (SLICE) method which can be used to form liquid metal particles of various sizes, shapes, compositions and surface morphologies.

Recently Hirano et al. reported a method using flame-assisted spray pyrolysis with a reducing gas atmosphere that yields high crystallinity pure hexagonal cesium tungsten bronze ($Cs_{0.32}WO_3$) nanoparticles which act as near-infrared shield in solar control windows to reduce energy consumption of air-conditioning [32]. Their method showed noteworthy near-infrared shielding ability with a 97.7% cut-off at 1500nm. Daza et al. investigated Cesium nanoparticles for cancer treatment therapy as an alternative of Cesium Chloride salts [28].

Yang et al. investigated optical properties of Cesium doped ZnO nanoparticles for solar cells applications that exhibit potential for low-cost and large-scale production with stable performance over three months storage under ambient conditions [33]. Cesium acts as an efficient electron layer in quantum dots solar cells.

Zhang et al. studied the effect of incorporation of Rubidium nanoparticles in perovskite solar cells using gas-quenching method and found that 5% amount of rubidium improves the efficiency of device and gives best performance extending the shell-life of device to one month in ambient conditions [34]. Albella et al. simulated plasmonic scattering by spherical and hemispherical Ga nanoparticles placed over dielectric surface [35]. The plasmonic spectra for various particle size and shape was studied as a function of illumination angle and polarization state (S-polarized and P-polarized) and their study lay the foundation for multiparticle system analysis in UV plasmonic devices.

Afresh study to control phase-change plasmonics in liquid and solid phases of gallium is reported by Gutiérrez et al. [36]. They discussed propagating and localized surface plasmon resonances in gallium nanostructures later to be implemented in plasmonics and photonic applications. Yang et al. recently reported a method to remove oxide layer occurring naturally over liquid metal surface that often affects their applications [37]. The oxide layer often influences the surface viscosity and adherent liquid metal properties. Boiling NaOH solution treatment was applied to remove the native oxide layer of liquid metal droplet. Reineck et al. discussed plasmonic response of liquid metal alloy eutectic gallium-indium (EGaIn) nanoparticles experimentally [38]. Their results showed plasmonic properties in UV region of electromagnetic spectrum. The work presented over the idea of reconfigurable liquid metal plasmonics which includes tuning of plasmonic response of particles by deforming the shape of nanoparticles. The scope of stretchable electronics with integration of liquid plasmonics with electronics was stated.

Tang et al. studied the phase behavior of gallium based liquid metal alloy (EGaIn) at micro- and nano- size scale [39].

The optical properties of gallium alloy nanoparticles before and after phase separation using in-situ spectroscopy were investigated. The stated their study as a starting point to engineer core-shell nanoparticles from liquid metals and also further scope for investigating properties and applications of them. Wang et al. used plasmonic response of liquid metal alloy to engineer reconfigurable plasmonic devices [40]. The enhanced transmission properties of eutectic gallium indium were applied to develop active devices which can also operate in other regions of electromagnetic spectrum. They stated it to be the first step to form more complex reconfigurable plasmonic devices.

4. Methodology

The understanding for interaction of incident light with metal NPs is required to study their plasmonic response. When light incidents on metal NPs the collective oscillation of conducting electrons takes place. This interaction leads to scattering of light by NP and also absorbing some part of it that accounts for energy loss. These energy losses in form of scattering and absorption efficiencies are calculated by methods discussed below:

Mie Theory: Mie in 1908 provided a complete theory of scattering and absorption of incident electromagnetic radiation by nanoparticles in spherical shape. The theory provides exact solutions of Maxwell equations for interaction of light and nanospheres in terms of infinite series with certain boundary conditions implemented on it. The quasi-static results for sub-wavelength spheres were evaluated by power series expansion of scattering and absorption coefficients of incident plane-wave. The theory was further extended to study the multilayer nanosphere as core-shell nanostructures [41]. The relations for inhomogeneous nanospheres are given below, a_n and b_n are Mie scattering coefficients for coated spherical core which are defined as,

$$a_n = \frac{\varphi_n(y)[\varphi_n'(n_2y) - A_n\chi_n'(n_2y)] - n_2\varphi_n'(y)[\varphi_n(n_2y) - A_n\chi_n(n_2y)]}{\xi_n(y)[\varphi_n'(n_2y) - A_n\chi_n'(n_2y)] - n_2\xi_n'(y)[\varphi_n(n_2y) - A_n\chi_n(n_2y)]},$$

$$b_n = \frac{n_2\varphi_n(y)[\varphi_n'(n_2y) - B_n\chi_n'(n_2y)] - \varphi_n'(y)[\varphi_n(n_2y) - B_n\chi_n(n_2y)]}{n_2\xi_n(y)[\varphi_n'(n_2y) - B_n\chi_n'(n_2y)] - \xi_n'(y)[\varphi_n(n_2y) - B_n\chi_n(n_2y)]},$$

Where A_n and B_n are derived from following relations,

$$A_n = \frac{n_2\varphi_n(n_2x)\varphi_n'(n_1x) - n_1\varphi_n'(n_2x)\varphi_n(n_1x)}{n_2\chi_n(n_2x)\varphi_n'(n_1x) - n_1\chi_n'(n_2x)\varphi_n(n_1x)}$$

$$B_n = \frac{n_2\varphi_n(n_1x)\varphi_n'(n_2x) - n_1\varphi_n(n_2x)\varphi_n'(n_1x)}{n_2\chi_n'(n_2x)\varphi_n(n_1x) - n_1\chi_n(n_2x)\varphi_n'(n_1x)}$$

Here, n_1 and n_2 are refractive indices of core and shell materials relative to surrounding medium. x = kR_{core} and y = kR_{shell} are size parameters, φ, φ', ξ, ξ' are Riccatti-Bessel functions and their derivatives [41]. According to Mie calculations, absorption and scattering efficiencies as a function of wavelength of homogenous spherical particles are given by,

$$Q_{ext} = \frac{2}{x_L^2}\sum_{n=1}^{\infty}(2n+1)Re\{a_n + b_n\},$$

$$Q_{sca} = \frac{2}{x_L^2}\sum_{n=1}^{\infty}(2n+1)(|a_n|^2 + |b_n|^2)$$

$$Q_{abs} = Q_{ext} - Q_{sca}$$

The layers of the inhomogeneous nanosphere (core-shell) is characterized by a size parameter $x_l = 2\pi n_m r_l/\lambda = kr_l$ with l= 1, 2,..., L and λ is the wavelength of the incident wave, r_l is the outer radius of the lth layer, k is the propagation constant, and n_m is the refractive index of the medium outside the particle.

Ovidio Pena-Rodriguez et al. [41] has provided a computer code based on Mie Theory which simulates optical properties of multi-layered nanoparticles of spherical geometry. The code is freely available and takes less time and is also validatory provides the same results as given by other methods. There are various methods like Finite Element Method, Boundary Element Method, Descrete Dipole Approximation, Finite Difference Time Domain Method [42-46]. All these methods provide solution to Maxwell equations for light interaction of nanoparticles and simulates optical properties for various particle shapes, sizes and surrounding optical medium. Nowadays, the most widely used numerical methods are DDA and FDTD methods for arbitrary shapes. The Maxwell curl equations are as follows:

$$\nabla \times E = -\frac{\partial B}{\partial t} \text{ and } \nabla \times B = \mu\epsilon\frac{\partial E}{\partial t}$$

Electromagnetic waves propagate through medium with a speed, v=c/n where n is the index of refractions for materials also known as ratio of speed of light in vacuum to speed of light in material medium given as, $n=\sqrt{\frac{\mu\epsilon}{\mu_0\epsilon_0}}$. The complex refractive index n of material describes the optical absorption and affected speed of EM light through medium. the imaginary part of it accounts for absorption of EM waves propagating through medium and the real part of the refractive index quantifying the lowering of phase velocity of propagating EM waves due to polarization of material medium.

Discrete Dipole Approximation (DDA) method: The DDA method was originally proposed by Purcell and Pennypacker in 1973 and was further reviewed and developed by Draine et al. [47, 45]. The DDA method calculates the absorption and scattering efficiencies of particles with arbitrary shapes such as rods, disks, cylinders, spheroids etc. The size of geometry is characterized by effective radius $r_{eff}=(3V/4\pi)^{1/3}$ where V is the volume of target material. The accuracy of DDA simulations depends on discretization step. The interparticle distance d must satisfy the condition |m|k. d≤1, where n is complex refractive index of target materials and k is wave number of light in propagating medium. the experimentally available data of target materials are introduced directly independent of the composition and geometry of material. The whole target is divided into array of N polarizable dipoles located on a cubic lattice with lattice spacing d. each dipole interacts with electromagnetic wave and exhibits polarizability, polarization given as:

$$P_j = \alpha_j E_j$$

where α is the polarizability and E is the electric field on jth dipole.

E_j is sum of incident field and re-radiated fields by other dipoles,

$$E_j = E_{inc,j} - \sum_{n=1}^{\infty} (A_{jk} P_k)$$

Here, A is the dipole-dipole interaction matrix. This equation is solved by Fast Fourier Transform method [48]. A computer code DDSCAT developed by Draine and Flatau provides fast calculations for solutions of arbitrary shaped particles [45, 47].

Finite Difference Time Domain (FDTD) method: The FDTD method solves Maxwell's equation in time domain using finite-difference approximations. The FDTD approach is easier to use and understand than other methods as it works by creating a movie of fields flowing through material of interest. The formulation of FDTD is based on Yee's cell and was first purposed by Kane S. Yee by studying the scattering of EM light by a perfectly conducting cylinder [49]. Later on, many studies were reported extending the FDTD approach to various areas of science and engineering [50-52]. The optical properties can be solved by FDTD method accordingly. The power absorbed per unit volume can be calculated from the divergence of Poynting vector

$$P_{abs} = -0.5\ \mathrm{Re}(\vec{\nabla}.\vec{S}) = -0.5\ \omega\ |E(\omega\omega)|^2\ \mathrm{Im}(\varepsilon(\omega)),$$

The absorption cross-section is defined as $C_{abs}(\omega) = \frac{P_{abs}(\omega\omega)}{I_{inc}(\omega\omega)}$,

where P_{abs} is the total power [W] absorbed by particle and I_{inc} is the incident source density [W/m^2]. Similarly, the scattered cross-section is defined as

$$C_{scat}(\omega) = \frac{P_{scat}(\omega\omega)}{I_{inc}(\omega\omega)}$$

where P_{scat} is the total power [W] scattered by particle. The total power scattered can be calculated by summing the power flowing outward through the four power monitors located in scattered field region of Simulation Area. The extinction cross-section is the sum of the absorption and scattering cross-sections,

$$C_{ext}(\omega) = C_{scat}(\omega) + C_{abs}(\omega).$$

5. Discussion

The study of optical properties of noble metal assisted-liquid metal nanoparticles will provide multifunctionality to plasmonic response of liquid metals and also makes them chemically stable to some extent which they lack off. The plasmonic response of some liquid metal alloys eutectic gallium indium (EGaIn) for the development of active devices to be functioned over wide region of electromagnetic spectrum has been reported [39, 40]. Also, many experimental and theoretical studies have been carried out for synthesization of gallium-based alloys such as gallinstan but as per our knowledge, no study is reported for the plasmonic behavior of elemental liquid metals and their alloys. Building on the work stated above, we started to see the new sights for liquid metals and liquid alloys on behalf of their LSPR based plasmonic properties. Hence, with the enhancement in plasmonic response of noble metal coated liquid metals and their alloys core-shell nanoparticles due to their liquid state at or near room temperature are interesting options for various applications like soft and stretchable electronics, optics, microfluidics, tunable and reconfigurable plasmonic devices. The LSPR based optical properties are reactive to even a minute change in the size, shape, and composition of metal nanoparticle and surrounding medium explained above. Thus, idea is to obtain the plasmonic response of liquid metal nanoparticles and their alloys in core-shell nanostructures.

6. Conclusions

The optical properties of metal nanoparticles can be studied by use of Mie Theory and Gans Theory which are based on solutions of Maxwell Equation for light interaction with nanoparticles. The incorporation of liquid metal nanoparticles in plasmonics can provide unique optical properties towards sensing and absorption-based applications where devices can become wearable due to flexibility provided by liquid phase nanoparticles. Dielectric functions are the most important response functions in condensed matter physics because of their deterministic role towards optical behavior of materials. The effect of electron oscillations with in metal nanoparticles providing localized surface plasmon resonance (LSPR), the calculation of extinction spectra (simulated by DDA and FDTD method) and simulating local field enhancements of metal nanoparticles which offer various applications of this research area. Despite widely exploited noble metals such as gold and silver, investigating the optical properties of new materials that are Noble metal assisted-liquids at room temperature paves a way to devices contributing to new applications.

References

[1] I. Freestone, N. Meeks, M. Sax, C. Higgitt, *Gold bulletin*. 40 (4), 270-277 (2007).

[2] M. Faraday, *X.* 147, 145-181 (1857).

[3] G. Mie, *Ann. Phys.* 25, 377 (1908).

[4] S. Link, M. B. Mohamed, M. A. El-Sayed, *J. Phys. Chem. B*. 103, 3073-3077 (1999).

[5] S. A. Maier, Plasmonics: fundamentals and applications, Springer Science & Business Media, Springer US 2007.

[6] J. S. Sekhon, S. S. Verma, *Plasmonics*. 6 (2), 311-317 (2011).

[7] S. Y. Shim, D. K. Lim, J. M. Nam, *Nanomedicine*. 3, 215–232 (2008).

[8] L. Wu, H. S. Chu, W. S. Koh, E. P. Li, *Optics express*. 18 (14), 14395-14400 (2010).

[9] G. Han, P. Ghosh, V. M. Rotello, *Nanomedicine*. 2, 113–123 (2007).

[10] V. Zharov, E. Galanzha, E. Shashkov, N. Khlebtsov, V. Tuchin, *Opt. Lett.* 31, 3623–3625 (2006).

[11] M. W. Knight, N. S. King, L. Liu, H. O. Everitt, P. Nordlander, N. J. Halas, *ACS nano*. 8 (1), 834-840 (2013).

[12] P. C. Wu, T. H. Kim, A. S. Brown, M. Losurdo, G. Bruno, H. O. Everitt, *Applied Physics Letters.* 90 (10), 103119 (2007).

[13] J. M. Sanz, D. Ortiz, R. Alcaraz De La Osa, J. M. Saiz, F. González, A. S. Brown, F. Moreno, *The Journal of Physical Chemistry C.* 117 (38), 19606-19615 (2013).

[14] S. Hayashi, T. Okamoto, *Journal of Physics D: Applied Physics.* 45 (43), 433001 (2012).

[15] C. Noguez, *The Journal of Physical Chemistry C.* 111 (10), 3806-3819 (2007).

[16] K. L. Kelly, E. Coronado, L. L. Zhao, G. C. Schatz, *J. Phys. Chem. B.* 107 (3) 668-677 (2003).

[17] L. Gao, Y. Zhang, V. Malyarchuk, L. Jia, K. I. Jang, R. C. Webb, D. Shah, (2014). *Nature communications.* 5, 4938.

[18] M. A. H. Khondoker, D. Sameoto, *Smart Materials and Structures.* 25 (9), 093001 (2016).

[19] T. Daeneke, K. Khoshmanesh, N. Mahmood, I. A. De Castro, D. Esrafilzadeh, S. J. Barrow, K. Kalantar-Zadeh, *Chemical Society Reviews.* 47 (11), 4073-4111 (2018).

[20] W. B. Jensen, *Journal of Chemical Education.* 80 (8), 952 (2003).

[21] D. R. Lide, (Ed.). CRC handbook of chemistry and physics (Vol. 85). CRC press 2004.

[22] V. Heine, *Journal of Physics C: Solid State Physics.* 1 (1), 222 (1968).

[23] M. Zhang, S. Yao, W. Rao, J. Liu, *Materials Science and Engineering: R: Reports.* 138, 1-35 (2019).

[24] Q. Wang, Y. Yu, K. Pan, J. Liu, *IEEE Transactions on Biomedical Engineering.* 61 (7), 2161-2166 (2014).

[25] B. F. Soares, F. Jonsson, N. I. Zheludev, *Physical review letters.* 98 (15), 153905 (2007).

[26] K. R. Nemade, S. A. Waghuley, *Applied Nanoscience. 7* (8), 753-758 (2017).

[27] P. Laurent, P. Lemonde, E. Simon, G. Santarelli, A. Clairon, N. Dimarcq, C. Salomon, *Eur. Phys. J. D.* 3 (3), 201-204 (1998).

[28] E. A. Daza, S. K. Misra, A. S. Schwartz-Duval, A. Ohoka, C. Miller, D. Pan, *ACS applied materials & interfaces*. 8 (40), 26600-26612 (2016).

[29] R. G. Chaudhuri, S. Paria, *Chemical reviews.* 112 (4), 2373-2433 (2011).

[30] P. C. Wu, M. Losurdo, T. H. Kim, B. Garcia-Cueto, F. Moreno, G. Bruno, A. S. Brown, *J. Phys. Chem. C.* 115 (28), 13571-13576 (2011).

[31] I. D. Tevis, L. B. Newcomb, M. Thuo, *Langmuir.* 30 (47), 14308-14313 (2014).

[32] T. Hirano, S. Nakakura, F. G. Rinaldi, E. Tanabe, W. N. Wang, T. Ogi, *Advanced Powder Technology.* 29 (10), 2512-2520 (2018).

[33] F. Yang, Y. Xu, M. Gu, S. Zhou, Y. Wang, K. Lu, Z. Wu, *J. Mater. Chem. A*, 6 (36), 17688-17697 (2018).

[34] M. Zhang, J. S. Yun, Q. Ma, J. Zheng, C. F. J. Lau, X. Deng, S. Huang, *ACS Energy Lett.* 2 (2), 438-444 (2017).

[35] P. Albella, B. Garcia-Cueto, F. González, F. Moreno, P. C. Wu, T. H. Kim, G. Videen, *Nano Lett.* 11 (9), 3531-3537 (2011).

[36] Y. Gutiérrez, M. Losurdo, P. García‐Fernández, M. Sainz de la Maza, F. González, A. S. Brown, F. Moreno, *Advanced Optical Materials.* 7 (13) 1900307 (2019).

[37] L. Yang, X. Zhao, S. Xu, Y. Lu, H. Chang, J. Liu, *Science China Technological Sciences.* (2019).

[38] P. Reineck, Y. Lin, B. C. Gibson, M. D. Dickey, A. D. Greentree, I. S. Maksymov, (2019). *Scientific reports.* 9 (1), 5345.

[39] S. Y. Tang, D. R. Mitchell, Q. Zhao, D. Yuan, G. Yun, Y. Zhang, W. Li, *Matter.* 1 (1), 192-204 (2019).

[40] J. Wang, S. Liu, A. Nahata, *Optics express.* 20 (11), 12119-12126 (2012).

[41] O. Peña-Rodríguez, P. P. González Pérez, U. Pal, *International Journal of Spectroscopy.* vol. 2011, Article ID 583743, 10 pages, (2011).

[42] M. I. Mishchenko, J. W. Hovenier, L. D. Travis, Meas. Sci. Technol. 11 (1827), (2000).

[43] P. Monk, Finite element methods for Maxwell's equations. Oxford University Press (2003).

[44] A. Buffa, M. Costabel, C. Schwab, *Numerische Mathematik.* 92 (4), 679-710 (2002).

[45] B. T. Draine, P. J. Flatau, *JOSA A.* 11 (4), 1491-1499 (1994).

[46] S. D. Gedney, Synthesis Lectures on Computational Electromagnetics, Morgan & Claypool, 6 (1), 1-250 (2011).

[47] B. T. Draine, P. J. Flatau, *JOSA A*. 25 (11), 2693-2703 (2008).

[48] J. J. Goodman, B. T. Draine, P. J. Flatau, *Optics Letters*. 16 (15), 1198-1200 (1991).

[49] K. Yee, *IEEE Transactions on antennas and propagation.* 14 (3), 302-307 (1966).

[50] M. N. Sadiku, *Numerical techniques in electromagnetics*. CRC press 1992.

[51] K. S. Kunz, R. J. Luebbers, The finite difference time domain method for electromagnetics. CRC press 1993.

[52] A. Taflove, Advances in computational electromagnetics. Artech House, Norwood, MA 1998.